RESEARCH PAPER

Acta Neurobiol Exp 2023, 83: 246–254
DOI: 10.55782/ane-2023-2429

IL-4 alleviates CIRI by suppressing autophagy *via* the HIF-1α/Bcl-2/BNIP3 pathway in rats

Yijun Suo[1†], Lu Zhang[2†], Yuanhang Che[3*]

[1] Department of Neurology, Affiliated Hospital of Jiujiang University, Jiujiang, Jiangxi Province, China,
[2] Department of Rehabilitation Medicine, Sir Run Run Shaw Hospital, College of Medicine, Zhejiang University, Hangzhou, Zhejiang Province, China,
[3] China Coast Guard Hospital of the People's Armed Police Force, Jiaxing, Zhejiang Province, China,
[†] The two authors contributed equally to this study,
** Email: cheyhccgh@imau-edu.cn*

This paper was designed for delving into the mechanism adopted by interleukin-4 (IL-4) to relieve cerebral ischemia-reperfusion injury (CIRI) in rats *via* suppressing autophagy. Herein, rats stochastically fell into sham operation (sham), model (RI), model + IL-4 intervention (IL-4), model + HIF-1α inhibitor (2-methoxyestradiol, 2ME2) and model + IL-4 + 2ME2 (IL-4 + 2ME2) groups. Next, western blotting was utilized to examine the protein expressions of microtubule-associated protein 1 light chain 3 (LC3), p62, hypoxia-inducible factor 1-alpha (HIF-1α) and Bcl-2/adenovirus E1B 19 kDa-interacting protein 3 (BNIP3). Relative to RI group, IL-4 group had a significantly lower neurological impairment scale (NIS) score and an overtly lower apoptosis rate of neurons as well as a strikingly smaller cerebral infarction volume and number of autophagosomes ($P<0.05$). The LC3II/LC3I ratio and HIF-1α and BNIP3 protein expressions dropped, but p62 protein expression rose pronouncedly in IL-4 group ($P<0.05$). In contrast to those in RI group, the NIS score, neuronal apoptosis rate, cerebral infarction volume and autophagosome number were strikingly reduced ($P<0.05$). The NIS score, cerebral infarction volume, neuronal apoptosis rate, autophagosome number, LC3II/LC3I ratio and protein expressions of HIF-1α and BNIP3 plummeted, while p62 protein expression sharply rose in IL-4 + 2ME2 group relative to those in IL-4 group ($P<0.05$). IL-4 suppresses cell autophagy by inhibiting the HIF-1α/BNIP3 pathway, thus relieving CIRI in rats.

Key words: IL-4, autophagy, HIF-1α, BNIP3, CIRI

INTRODUCTION

Cerebrovascular diseases appear to be the second major cause of death around the globe, and the first killer in China. Among all cerebrovascular diseases, ischemic stroke accounts for about 80%, occupying the dominant position (Saw et al., 2019). Generally, ischemic diseases are currently treated by thrombolysis in clinical practice, but the restoration of blood flow during the treatment is likely to bring secondary injury to the injured tissues, namely, cerebral ischemia-reperfusion injury (CIRI), which involves an array of pathological changes such as oxidative stress, inflammation, autophagy, apoptosis, and endoplasmic reticulum stress (Liu et al., 2021). It has been demonstrated by some scholars that autophagy is essential for CIRI (Xu et al., 2021). As an anti-inflammatory cytokine, interleukin-4 (IL-4), by virtue of its own receptors, affects the differentiation of mononuclear macrophages, increases the secretion of anti-inflammatory cytokines, and hinders TNF-α and other inflammatory cytokines to be released, so as to achieve anti-inflammation (Lee et al., 2020). In addition, IL-4 suppresses excessive autophagy, alleviates CIRI in mice, and enhances the long-term cognitive function to protect the brain, but

Received 1 March 2023, accepted 13 June 2023

its mechanism in inhibiting autophagy needs to be explored (Li et al., 2020). Autophagy is a catabolic process of important materials in eukaryotic cells, which exists conservatively and is maintained at a proper level. It can be used to remove damaged organelles and misfolded cells in the body, and effectively meets the needs of cells for efficient and stable metabolism (Singla et al., 2020).

Nonetheless, excessive autophagy in the body is not beneficial for the maintenance of cell stability and aggravates cell injury to trigger cell death. This type of death is programmed, so it is often called autophagic cell death or programmed cell death (Wang et al., 2020). Hypoxia-inducible factor 1-alpha (HIF-1α) is the main transcriptional regulator of the cellular response to hypoxia and also a major pathway involved in neuroprotection (Scatozza et al., 2020). Bcl-2/adenovirus E1B 19 kDa-interacting protein 3 (BNIP3), as a receptor for mitophagy, induces autophagy by directly binding LC3 (Xie et al., 2020). It has been reported that HIF-1α can affect the apoptosis of brain cells by inducing BNIP3 expression (Zhu et al., 2019). However, the action mechanism of HIF-1α and BNIP3 in CIRI remains elusive.

On this account, the action mechanism adopted by IL-4 to suppress autophagy through regulating the HIF-1α/BNIP3 signaling pathway to reduce CIRI is the research objective herein.

METHODS

Animals

A total of 50 SPF-grade male Sprague-Dawley rats [Laboratory Animal Center of Medical College of China Three Gorges University, License No. SCXK (Hubei) 2011-0012, China], weighing 250-280 g, were all fed in an animal house exposed to 12-h shift of the light-dark cycle at 18-26°C and 40-70% relative humidity, with continuous ventilation (8-12 times per hour). They were all adaptively fed for one week with ad libitum feeding. This study has been approved by the animal ethics committee of our hospital (approval No. CCGH2020013), and great efforts have been made to minimize the animals' suffering.

Amyjet Scientific Co., Ltd. (China) provided rat anti-mouse IL-4 neutralizing antibody and recombinant mouse IL-4 antibody, BOSTER Biological Technology Co., Ltd. (China) provided goat anti-rabbit glyceraldehyde 3-phosphate dehydrogenase antibody, Abcam (USA) offered rabbit anti-polyclonal autophagy marker microtubule-associated protein 1 light chain 3 (LC3) antibody, Cell Signaling Technology (USA) offered antibodies against rabbit anti-polyclonal p62 and mouse anti-HIF-1α and BNIP3, Santa Cruz (USA) offered horseradish peroxidase-labeled goat anti-mouse IgG antibody, Selleck (USA) provided HIF-1α inhibitor 2-methoxyestradiol (2ME2), Nanjing Jiancheng Bioengineering Institute (China) provided triphenyl tetrazolium chloride staining solution, and Wuhan Saipei Biotechnology Co., Ltd. (China) offered terminal deoxynucleotidyl transferase dUTP nick end labeling (TUNEL) kit.

Preparation of IL-4 complex solution (IL-4C): At the mass ratio of 1:5, the mixture of rat anti-mouse IL-4 neutralizing antibody (50 μg) and recombinant mouse IL-4 antibody (10 μg) underwent dilution to 50 mg/mL using physiological saline with 1% rat serum. The rats stochastically fell into sham operation group (sham group, undergoing intraperitoneal injection of normal saline with the same volume as that in drug groups at 30 min before modeling), model group (RI group, receiving intervention with the same drug as that in sham group), model + IL-4 intervention group (IL-4 group, undergoing intraperitoneal injection of 0.2 mL of IL-4C for intervention at 30 min before modeling), model + HIF-1α inhibitor group (2ME2 group, receiving intraperitoneal injection of 15 mg/kg 2ME2 at 30 min before modeling), and model + IL-4 + 2ME2 group (IL-4 + 2ME2 group, receiving intraperitoneal injection of 0.2 mL of IL-4C + 15 mg/kg 2ME2 at 30 min before modeling), with 10 rats per group.

Modeling

As per the Longa method, the rat right middle cerebral artery occlusion was modelled. Specifically, the rats were anesthetized at 30 min after the last administration and fixed in the supine position to make the rats' neck fully exposed. Then a 2-cm long incision was made along the midline after disinfection, followed by separation and full exposure of the common carotid artery, external carotid artery and internal carotid artery successively. Next, the common carotid artery and internal carotid artery were temporarily clamped with aortic clips, and the external carotid artery was cut with a "V" shape. Later, the aortic clips at the internal carotid artery were removed. The thread knot prepared in advance was inserted into the neck from the external carotid artery until there was slight resistance. At this time, the thread knot exactly occluded the incision of the middle cerebral artery. At 1 h after occlusion of the left incision, the thread knot was pulled out, the artery stump was ligated, and the skin received layer-by-layer suture. In sham group, the arteries of rats were only isolated, without thread knot insertion and ligation.

Subsequent to 24 h modeling, the NIS score of each group of rats was assessed as follows: 0 points: normal neurological function, 1 point: incomplete flexion or stretching of the left forelimb when being lifted by the tail, 2 points: leftward circling or rear-end collision during walking, 3 points: walking difficulty and leftward-twisting tendency of the body during walking, and 4 points: inability to walk or unconsciousness. The score obtained by the rats ranging 1-3 points meant the successful establishment of the RI model. All the rats with scores of 0 and 4 points were excluded, and 10 rats in each group should be guaranteed.

Subsequent to 24 h RI, the anesthesia by 1.5 mL of 10% chloral hydrate and decapitation were stochastically performed in each group. After that, the brain was taken out, and the olfactory bulb, cerebellum and low-grade brain stem in the brain tissues were discarded, respectively. Then the rats were frozen in the refrigerator at -20°C for 20 min. Next, the rats were taken out, and the brain tissues were cut into 5 equal parts along the coronal plane and incubated in 0.2% triphenyl tetrazolium chloride staining solution in phosphate-buffered saline (0.1 mol/L) for half an hour away from light, followed by 24 h fixation in 4% formaldehyde polycondensation solution. Later, the brain tissues were taken out and sliced, and the residue solution was sucked away. Finally, the brain tissues were photographed, and the cerebral infarction (CI) volume of all rats was analyzed using software.

Determination of apoptosis by TUNEL assay

Embedded in paraffin, the brain tissues of all rats were sliced into sections, and neuronal apoptosis was determined *via* TUNEL assay in each group. In detail, the brain tissue sections underwent de-paraffinization and 20-min incubation with 2% protease K at indoor temperature. Subsequent to rinsing with phosphate-buffered saline, 1 h section incubation with TUNEL reaction mixture (50 μL) was completed in a wet box. After mounting by anti-fluorescence quenching solution, the number of apoptotic neurons showing green fluorescence was observed under a fluorescence microscope.

Detection of autophagosomes using transmission electron microscopy

At 24 h following RI, some rats in each group were anesthetized and perfused with normal saline. When the liver and forelimbs of the rats turned white, the rats were further perfused with 4% paraformaldehyde-2.5% glutaraldehyde solution (Thermo Fisher Scientific, USA). After successful perfusion, the brain was taken from the rats by decapitation, and the brain tissues were separated. A brain tissue block with a volume of about 1 mm^3 was taken from the ischemic hippocampus near CA1 area and stored in 2.5% glutaraldehyde solution for fixation. Then the fixed brain tissue block was washed with phosphate-buffered saline thrice, and fixed in 1% osmium tetroxide solution (Sigma-Aldrich, USA) at 4°C for 1 h. Subsequently, the tissue block fixed in osmium tetroxide solution was dehydrated using gradient ethanol, embedded in epoxy resin, and polymerized at -80°C for 24 h. Later, the tissue block was sliced into 60-70-nm thick sections by an ultramicrotome, and stained with 3% lead citrate. At last, transmission electron microscopy (Thermo Fisher Scientific, USA) was conducted for observation of the autophagosomes formed.

Measurement of protein expressions of LC3, p62, HIF-1α and BNIP3 by western blotting

A total of 50 mg brain tissues were collected from rats in each group, and cut and lysed on ice. Subsequent to 10-min centrifugation at 4°C and 12,000 r/min, BCA assay was implemented for measurement of the total protein concentration in the supernatant. Specifically, the protein was loaded *via* 12% SDS-PAGE for membrane transfer and underwent 1 h blocking in 5% non-fat milk. Next, the protein received 1 h incubation with primary antibodies against LC3 (1:500), p62 (1:500), HIF-1α (1:500) and BNIP3 (1:500) at 4°C for 1 h, and 1 h incubation with horseradish peroxidase-labeled secondary antibody (1:10,000) at indoor temperature, followed by rinsing with TBST. All bands were observed using ECL kit (Thermo Fisher Scientific, USA), and ImageJ software (National Institutes of Health, USA) was adopted for the analysis of the band density, with β-actin as the internal reference.

Statistical analysis

Prism 8.0 software (GraphPad, USA) was utilized for statistical analysis. Mean ± standard deviation ($\overline{x} \pm s$) was adopted to present the NIS score, CI volume, neuronal apoptosis, number of autophagosomes and the protein expressions of LC3, p62, HIF-1α and BNIP3. Intergroup comparison was performed by the t test. One-way analysis of variance was employed to compare the differences among three groups, and the LSD-t test was conducted for pairwise comparison between two groups. A difference appeared to be statistically significant in the case of P value below 0.05.

RESULTS

Effects of IL-4 on neurological impairment score, cerebral infarction volume, neuronal apoptosis rate and formation of autophagosomes

Relative to those in sham group, the NIS score, CI volume and neuronal apoptosis rate in RI group markedly rose (LSD-$t_{NIS\ score}$=22.86, LSD-$t_{CI\ volume}$=22.42, LSD-$t_{neuronal\ apoptosis\ rate}$=21.38, P<0.0001), and these indicators were markedly reduced in IL-4 group in contrast to those in RI group (LSD-$t_{NIS\ score}$=13.23, LSD-$t_{CI\ volume}$=8.63, LSD-$t_{neuronal\ apoptosis\ rate}$=10.83, P<0.0001) (Fig. 1A-E and Table 1).

In sham group, neurons in the ischemic area CA1 of brain tissues in rats were relatively normal, with relatively complete nuclei, mitochondria, and lysozymes. In RI group, the rats showed destroyed cell morphology in the ischemic area CA1 of brain tissues, with many vacuoles, lysozymes and autophagosomes in neurons. Compared with those RI group, the number of autophagosomes in the area CA1 of rats was markedly reduced, and the cell morphology was relatively normal, with relatively complete mitochondria, lysozymes and endoplasmic reticula in IL-4 group (Fig. 1F). Collectively, IL-4 improved the neurological function, reduced the volume of cerebral infarction and neuronal apoptosis rate, and inhibited the formation of autophagosomes, thereby alleviating CIRI in rats.

Effects of IL-4 on protein expressions of LC3, p62, HIF-1α and BNIP3 in brain tissues

In comparison with those in sham group, the LC3II/LC3I ratio and the protein expressions of HIF-1α and BNIP3 in the brain tissues pronouncedly rose, but the p62 protein expression strikingly plummeted in RI group (LSD-$t_{LC3II/LC3I\ ratio}$=21.37, LSD-t_{p62}=18.48, LSD-$t_{HIF\text{-}1\alpha}$=19.04, LSD-t_{BNIP3}=13.97, P<0.0001). Relative to RI group, IL-4 group displayed strikingly declined LC3II/LC3I ratio and protein expressions of HIF-1α and BNIP3 and an evidently elevated protein expression of p62 in IL-4 group (LSD-$t_{LC3II/LC3I\ ratio}$=16.73, LSD-t_{p62}=11.55, LSD-$t_{HIF\text{-}1\alpha}$=15.90, LSD-t_{BNIP3}=5.69, P<0.0001) (Fig. 2 and Table 2). Therefore, IL-4 mitigated CIRI in rats possibly by inhibiting the HIF-1α/BNIP3 signaling pathway and promoting autophagy.

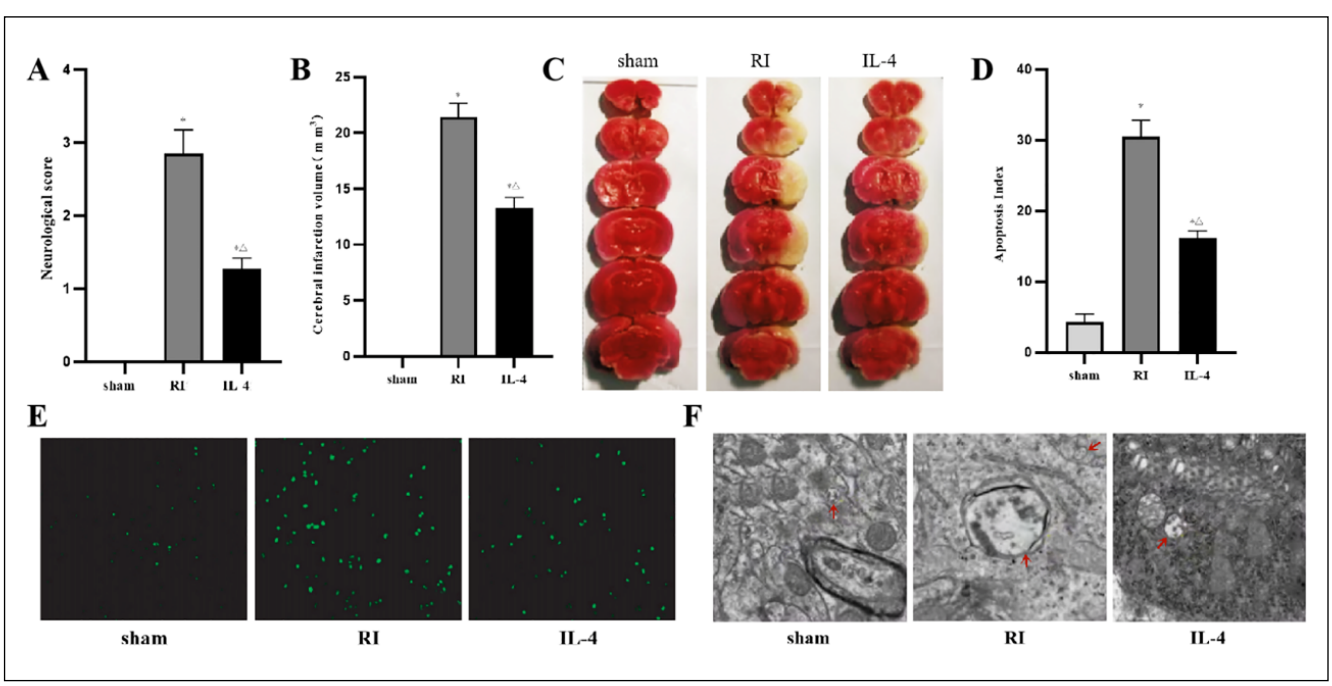

Fig. 1. Effects of IL-4 on neurological impairment score, cerebral infarction volume, neuronal apoptosis and autophagosome formation. (A) Neurological impairment score; (B) and (C) cerebral infarction volume; (D) and (E) neuronal apoptosis rate. Relative to those in sham group, the NIS score, CI volume and neuronal apoptosis rate in RI group markedly rose, and these indicators were markedly reduced in IL-4 group in contrast to those in RI group. F: autophagosome formation observed by transmission electron microscopy, with arrows indicating autophagosomes. Compared with those RI group, the number of autophagosomes in the area CA1 of rats was markedly reduced, and the cell morphology was relatively normal, with relatively complete mitochondria, lysozymes and endoplasmic reticula in IL-4 group. *P<0.05 *vs.* sham group and ΔP<0.05 *vs.* RI group. CI: Cerebral infarction; IL-4: interleukin-4; NIS: neurological impairment scale; RI: reperfusion injury.

Table 1. Neurological impairment score, cerebral infarction volume, neuronal apoptosis rate of different groups.

Group	Neurological score (point)	Cerebral infarction volume (mm^3)	Apoptosis index
Sham (n=10)	0	0	4.25±0.51
RI (n=10)	2.81±0.42*	22.57±3.18*	31.27±4.42*
IL-4 (n=10)	1.19±0.23*$^{\Delta}$	13.89±2.25*$^{\Delta}$	17.58±2.04*$^{\Delta}$
F	263.511	255.750	228.563
P	<0.001	<0.001	<0.001

*P<0.05 *vs.* sham group; $^{\Delta}$P<0.05 *vs.* RI group.

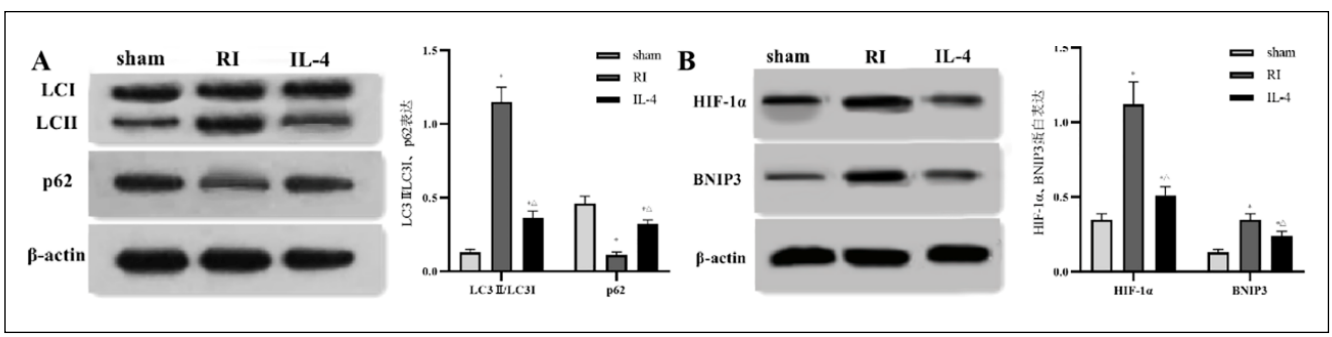

Fig. 2. Effects of IL-4 on protein expressions of LC3, p62, HIF-1α and BNIP3 in brain tissues. (A) LC3 and p62 protein expressions; (B) HIF-1α and BNIP3 protein expressions. In comparison with those in sham group, the LC3II/LC3I ratio and the protein expressions of HIF-1α and BNIP3 in the brain tissues pronouncedly rose, but the p62 protein expression strikingly plummeted in RI group. Relative to RI group, IL-4 group displayed strikingly declined LC3II/LC3I ratio and protein expressions of HIF-1α and BNIP3 and an evidently elevated protein expression of p62 in IL-4 group. *P<0.05 *vs.* sham group and $^{\Delta}$P<0.05 *vs.* RI group. BNIP3: Bcl-2/adenovirus E1B 19 kDa-interacting protein 3; HIF-1α: hypoxia-inducible factor 1-alpha; IL-4: interleukin-4; LC3: microtubule-associated protein 1 light chain 3; RI: reperfusion injury.

Table 2. Protein expressions of LC3, p62, HIF-1α and BNIP3 in brain tissues.

Group	LC3II/LC3I	p62	HIF-1α	BNIP3
Sham (n=10)	0.18±0.03	0.48±0.05	0.37±0.05	0.15±0.02
RI (n=10)	1.24±0.18*	0.16±0.02*	1.22±0.15*	0.42±0.06*
IL-4 (n=10)	0.41±0.06*$^{\Delta}$	0.36±0.04*$^{\Delta}$	0.51±0.07*$^{\Delta}$	0.31±0.04*$^{\Delta}$
F	252.764	174.222	208.395	98.750
P	<0.001	<0.001	<0.001	<0.001

*P<0.05 *vs.* sham group; $^{\Delta}$P<0.05 *vs.* RI group.

Effects of HIF-1α inhibitor 2ME2 on neurological impairment score, cerebral infarction volume, neuronal apoptosis rate and autophagosome formation

2ME2 group exhibited a lower neurological function score, a smaller CI volume, and a lower neuronal apoptosis rate than RI group (tNIS score=19.61, $t_{CI\ volume}$=9.69, $t_{neuronal\ apoptosis\ rate}$=25.54, P<0.0001) (Fig. 3A-E). In 2ME2 group, the number of autophagosomes in the area CA1 of rats declined remarkably, and the cell morphology was relatively normal, with relatively complete mitochondria, lysozymes and endoplasmic reticula (Fig. 3F). Thus, the HIF-1α inhibitor 2ME2 also improved the neurological function, decreased the cerebral infarct volume and neuronal apoptosis rate, and suppressed the formation of autophagosomes, then relieving CIRI in rats.

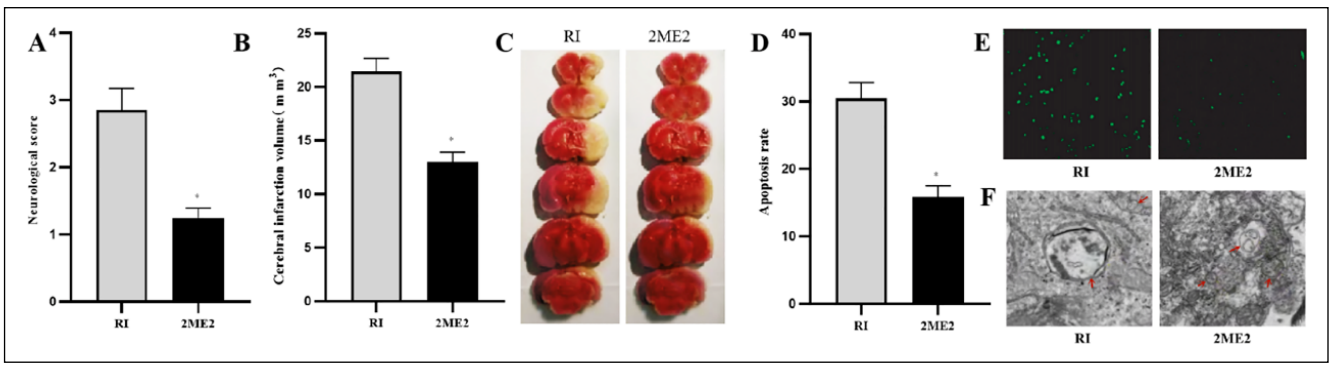

Fig. 3. Effects of HIF-1α inhibitor 2ME2 on neurological impairment score, cerebral infarction volume, neuronal apoptosis rate and autophagosome formation. (A) Neurological function score; (B) and (C) cerebral infarction volume; (D) and (E) neuronal apoptosis rate. 2ME2 group exhibited a lower neurological function score, a smaller CI volume, and a lower neuronal apoptosis rate than RI group. (F) autophagosome formation observed by transmission electron microscopy, with arrows indicating autophagosomes. In 2ME2 group, the number of autophagosomes in the area CA1 of rats declined remarkably, and the cell morphology was relatively normal, with relatively complete mitochondria, lysozymes and endoplasmic reticula. *P<0.05 *vs.* sham group. 2ME2: 2-Methoxyestradiol; CI: cerebral infarction; HIF-1α: hypoxia-inducible factor 1-alpha; RI: reperfusion injury.

Effects of HIF-1α inhibitor 2ME2 on protein expressions of LC3, p62, HIF-1α and BNIP3 in brain tissues

The LC3II/LC3I ratio showed a notable plunge, while the protein expression of p62 was evidently raised in 2ME2 group compared with those in RI group ($t_{LC3II/LC3I\ ratio}$=17.40, t_{p62}=9.19, P<0.0001). Besides, 2ME2 group had lower protein expressions of HIF-1α and BNIP3 relative to RI group ($t_{HIF\text{-}1\alpha}$=14.88, t_{BNIP3}=7.05, P<0.0001) (Fig. 4). Hence, the HIF-1α inhibitor 2ME2 also alleviated CIRI in rats probably by suppressing the HIF-1α/BNIP3 signaling pathway and facilitating autophagy.

Effects of IL-4 + 2ME2 on neurological impairment score, cerebral infarction volume, neuronal apoptosis rate and autophagosome formation

The NIS score, CI volume and neuronal apoptosis rate were markedly decreased in IL-4 + 2ME2 group in comparison with those in IL-4 group (tNIS score=2.63, $t_{CI\ volume}$=7.66, $t_{neuronal\ apoptosis\ rate}$=8.43, P<0.0001) (Fig. 5A-E). Additionally, the number of autophagosomes in the area CA1 was evidently decreased, and the cell morphology was relatively normal, with relatively complete mitochondria, lysozymes, and endoplasmic reticula in IL-4 + 2ME2 group in contrast to those in IL-4 group (Fig. 5F). Taken together, IL-4 in combination with the HIF-1α inhibitor 2ME2 mitigated CIRI in rats more effectively than IL-4 alone.

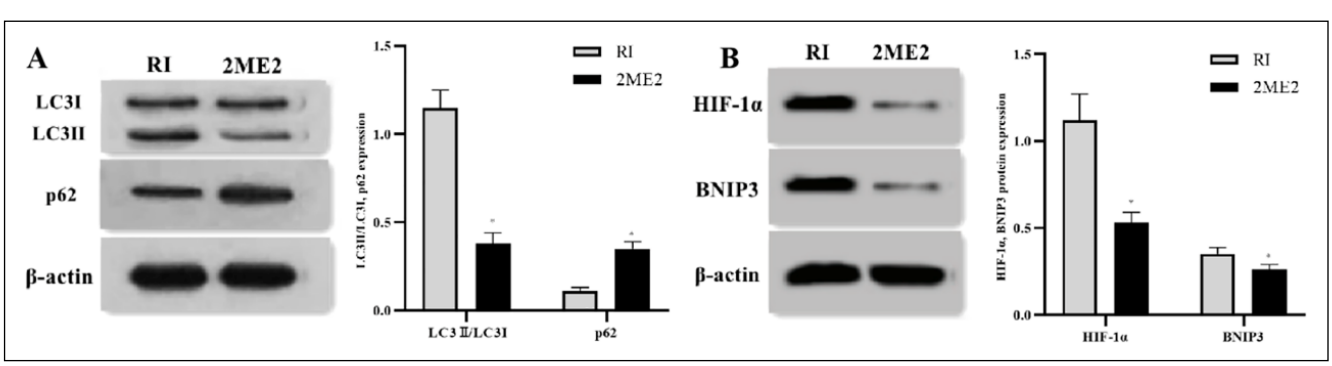

Fig. 4. Effects of HIF-1α inhibitor 2ME2 on protein expressions of LC3, p62, HIF-1α and BNIP3 in brain tissues. (A) LC3 and p62 protein expressions; (B) HIF-1α and BNIP3 protein expressions. The LC3II/LC3I ratio showed a notable plunge, while the protein expression of p62 was evidently raised in 2ME2 group compared with those in RI group. 2ME2 group had lower protein expressions of HIF-1α and BNIP3 relative to RI group. *P<0.05 *vs.* RI group. 2ME2: 2-Methoxyestradiol; BNIP3: Bcl-2/adenovirus E1B 19 kDa-interacting protein 3; HIF-1α: hypoxia-inducible factor 1-alpha; LC3: microtubule-associated protein 1 light chain 3; RI: reperfusion injury.

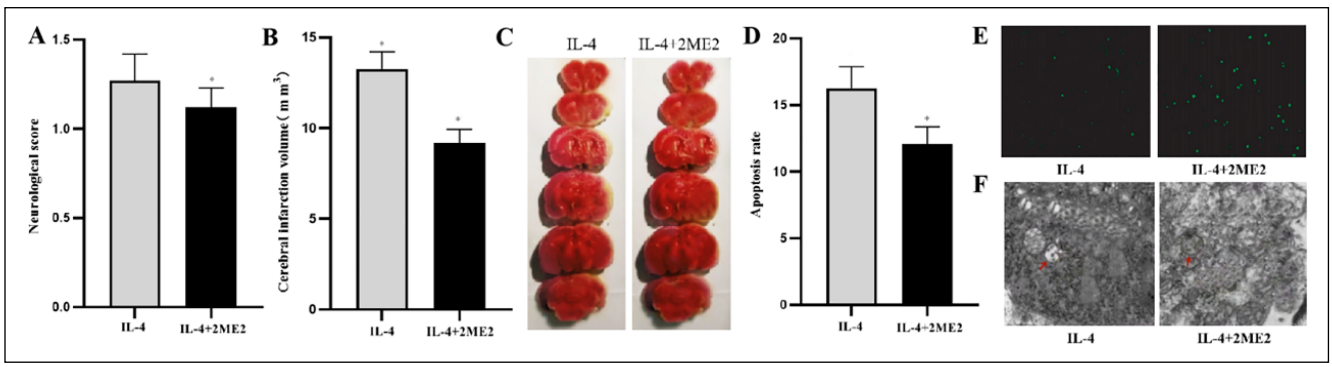

Fig. 5. Effects of IL-4 + 2ME2 on neurological function score, cerebral infarction volume, neuronal apoptosis rate and autophagosome formation. (A) Neurological function score; (B) and (C) cerebral infarction volume; (D) and (E) neuronal apoptosis rate. The NIS score, CI volume and neuronal apoptosis rate were markedly decreased in IL-4 + 2ME2 group in comparison with those in IL-4 group. F: autophagosome formation observed by transmission electron microscopy, with arrows indicating autophagosomes. The number of autophagosomes in the area CA1 was evidently decreased, and the cell morphology was relatively normal, with relatively complete mitochondria, lysozymes, and endoplasmic reticula in IL-4 + 2ME2 group in contrast to those in IL-4 group. *P<0.05 *vs.* IL-4 group. 2ME2: 2-Methoxyestradiol; CI: cerebral infarction; IL-4: interleukin-4.

Effects of IL-4 + 2ME2 on protein expressions of LC3, p62, HIF-1α and BNIP3 in brain tissues

Relative to those in IL-4 group, the ratio of LC3II/LC3I evidently dropped, whereas the protein expression of p62 overtly rose in the brain tissues of rats in IL-4 + 2ME2 group ($t_{LC3II/LC3I\ ratio}$=9.98, t_{p62}=7.05, P<0.0001). Moreover, IL-4 + 2ME2 group exhibited overtly lower protein expressions of HIF-1α and BNIP3 than IL-4 group ($t_{HIF\text{-}1\alpha}$=6.14, t_{BNIP3}=7.89, P<0.0001) (Fig. 6). In short, IL-4 combined with the HIF-1α inhibitor 2ME2 promoted autophagy by inhibiting the HIF-1α/BNIP3 signaling pathway, thereby relieving CIRI in rats. The combination worked significantly better than IL-4 alone. The results further confirmed that IL-4 alleviated CIRI in rats by regulating the HIF-1α/BNIP3 signaling pathway.

DISCUSSION

CIRI has a relatively complicated pathogenesis, which involves such pathological links as energy metabolism disorder, release of inflammatory mediators, free radical injury, induction of apoptosis and autophagy (Zhu et al., 2020). These pathological links intertwine with each other but do not exist independently, and they will ultimately lead to cell death, especially necrosis, apoptosis, autophagy and other types of programmed cell death, among which autophagy-related cell death has attracted considerable concern (Ling et al., 2021). Autophagy is a catabolic process involving lysosomes in eukaryotic cells, which degrades unfolded proteins, scavenges aging organelles and intracellular pathogens, and mediates cell homeostasis and energy

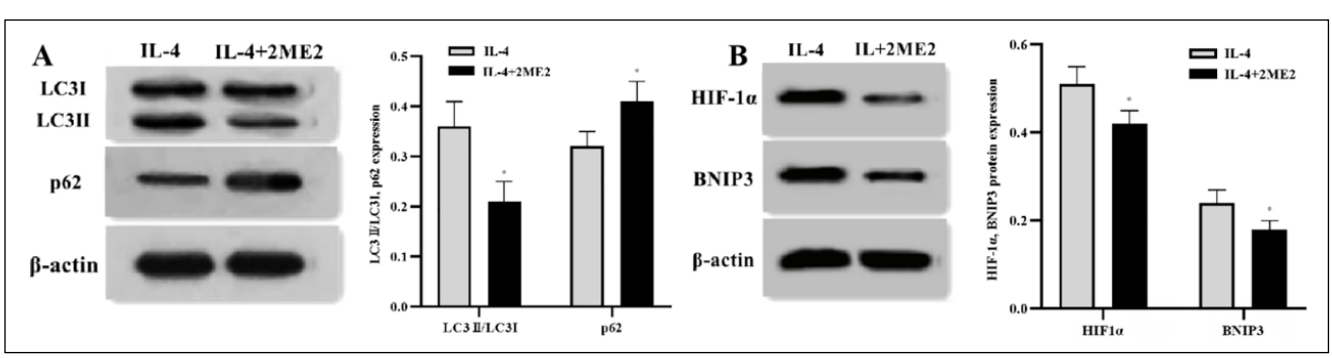

Fig. 6. Protein expressions of LC3, p62, HIF-1α and BNIP3 in brain tissues. (A) LC3 and p62 protein expressions; (B) HIF-1α and BNIP3 protein expressions. Relative to those in IL-4 group, the ratio of LC3II/LC3I evidently dropped, whereas the protein expression of p62 overtly rose in the brain tissues of rats in IL-4 + 2ME2 group. IL-4 + 2ME2 group exhibited overtly lower protein expressions of HIF-1α and BNIP3 than IL-4 group. *P<0.05 *vs.* IL-4 group. 2ME2: 2-Methoxyestradiol; BNIP3: Bcl-2/adenovirus E1B 19 kDa-interacting protein 3; HIF-1α: hypoxia-inducible factor 1-alpha; IL-4: interleukin-4; LC3: microtubule-associated protein 1 light chain 3.

metabolism (Shao et al., 2021). Moderate autophagy provides free fatty acids, amino acids and nucleotides and scavenges injured organelles to protect neurons. Nonetheless, the up-regulated autophagy for a long term will result in excessive degradation of cell contents, thus inducing cell death and aggravating CIRI (Yao et al., 2019). Excessive autophagy will aggravate CIRI (Wang et al., 2019). It has been recently found that the relationship between autophagy and inflammation affects the development of many diseases. The research on Crohn's disease revealed that inflammatory responses occur in the epithelium of the small intestine, and inflammatory cytokines mediate the autophagy of cells (Giudici et al., 2019).

HIF-1α is a cellular hypoxia-related transcription factor, and its up-regulation under hypoxic stress can activate multiple related pathways (Chaudhuri et al., 2020). However, its role and mechanism in hypoxic injury are still controversial, probably due to the specificity of cell types and concentration-related bidirectional regulation. The pathogenesis of ischemic-hypoxic injury is complex, and various molecular mechanisms can lead to neuronal apoptosis and necrosis. Accelerated neuronal apoptosis is the main factor of neurodegeneration. Hypoxia facilitates neuronal apoptosis, and also increases the expression of HIF-1α in neurons (Abdel-Latif et al., 2020). BNIP3 competes with Beclin-1 to destroy Beclin-1/Bcl-2 and Beclin-1/Bcl-XL complexes, thereby releasing Beclin-1 and enhancing autophagy (El-Ella et al., 2022). This study yielded that the protein expression of BNIP3 was positively associated with that of HIF-1α in rats in RI group. The occurrence process of autophagy involves the initiation of autophagy, the assembly and formation of autophagosomes, the binding of autophagosomes to lysosomes, and the substrate degradation by autophagy-associated lysosomes. This process called autophagic flux is dynamic, and the activation of autophagic flux is the prerequisite for autophagy to perform its biological function (Huang et al., 2019). In the present study, therefore, autophagosome formation was observed *via* transmission electron microscopy, and multiple autophagosome-like structures with bilayer membranes were observed in rats in RI group.

Besides, autophagy can be detected *via* the LC3II/LC3I ratio and the protein expression level of p62. LC3 is a vital autophagy marker and falls into type I that is commonly expressed and exists freely in the cytoplasm and type II. When autophagy occurs, LC3I combines with phosphatidylethanolamine to form LC3-PE, namely, membrane-binding LC3II. The membrane-binding LC3II, constantly present in the membrane of intracellular autophagosomes, has a concentration proportional to the number of autophagosomes. In addition, p62 is a connexin connecting ubiquitinated proteins to LC3, and also the substrate protein for autophagy. The aggregation of p62 reflects the degradation of autophagy-associated lysosomes, whereas the decline in p62 level reflects the completion of degradation by autophagy (Yang et al., 2019). It was found in this study that the LC3II/LC3I ratio rose but the protein expression of p62 dropped in rats in RI group, indicating that autophagy is up-regulated in cells during CIRI. A study has revealed that the HIF-1α/BNIP3 signaling pathway is dramatically enhanced after 24 h of cerebral ischemia-reperfusion, and its activation-induced autophagy may be beneficial in the early stage of cerebral ischemia-reperfusion, but excessive autophagy is harmful in the advanced stage of cerebral ischemia (Liu et al., 2019). 2ME2 is an inhibitor specific to HIF-1α, and its inhibitory role in the activation of the HIF-1α/BNIP3 signaling pathway and autophagy to alleviate CIRI has been proven (Zhang et al., 2019).

According to the results of this study, IL-4 protected the brain tissues of CIRI rats and down-regulated the NIS score, CI volume and neuronal apoptosis rate. Autophagy may play key roles in neuronal survival and death. However, the role of autophagy in CIRI is still controversial currently. Promoting autophagy is able to prevent CIR (Huang et al., 2019). In contrast, the others reported that autophagy activation during CIR helped to remove damaged organelles and promote the circulation of energy and substances, often as a protective mechanism. Nevertheless, excessive autophagy can aggravate neuronal apoptosis and necrosis. The detection results of protein expressions herein manifested that the intraperitoneal injection of IL-4 could down-regulate the LC3II/LC3I ratio but up-regulate the protein expression of p62 in the brain tissues of CIRI rats, suggesting that the mechanism of IL-4 in reducing CIRI is likely to be associated with the inhibition on excessive autophagy. The study of Mokhtari-Zaer et al. (2020) demonstrated that the learning and memory abilities of mice intraperitoneally injected with IL-4 obviously weakened, which may be attributed to excessive autophagy in mouse brain tissues.

Meanwhile, the current study also manifested that the protein expressions of HIF-1α and BNIP3 in the brain tissue in IL-4 group dropped, indicating that the mechanism of IL-4 in inhibiting the protection against excessive autophagy-induced CIRI is probably associated with the down-regulation of the HIF-1α/BNIP3 signaling pathway. In addition, no evident differences were detected between 2ME2 group and IL-4 group in NIS score, CI volume and neuronal apoptosis rate, as well as in the protein expressions of HIF-1α, BNIP3 and p62, and LC3II/LC3I ratio. Hence, it was speculated that IL-4 has a similar action mechanism as its inhibitor 2ME2, by which the two can suppress the HIF-1α/

BNIP3 signaling pathway and excessive autophagy, and protect against CIRI. Besides, the NIS score, CI volume and neuronal apoptosis rate, IL-4 + 2ME2 group displayed lower protein expressions of HIF-1α and BNIP3 and LC3II/LC3I ratio in but a higher protein expression of p62 relative to IL-4 group. The comparison results between the two groups confirmed the above findings. Xing et al. (2015) conducted research and proved that IL-4 can suppress autophagy by activating the Akt/GSK-3β signaling pathway to relieve CIRI in mice.

CONCLUSION

In summary, IL-4 exerts an inhibitory effect on cell autophagy through inhibiting the HIF-1α/BNIP3 signaling pathway, thus alleviating CIRI in rats and protecting their brain tissues. We postulate that IL-4 plays a protective role in the brain tissues of rats with CIRI by suppressing autophagy. The findings provide novel insights into the clinical treatment of CIRI. Regardless, this study is still limited. We herein only performed *in vivo* animal studies owing to low research budget, so the results may be biased. Future *in vitro* and clinical studies are ongoing in our group to provide more valuable evidence for the clinical treatment of CIRI.

ACKNOWLEDGEMENT

This study was financially supported by the Science and Technology Plan Project of Jiangxi Provincial Health Commission No. 202212006.

REFERENCES

Abdel-Latif RG, Rifaai RA, Amin EF (2020) Empagliflozin alleviates neuronal apoptosis induced by cerebral ischemia/reperfusion injury through HIF-1α/VEGF signaling pathway. Arch Pharm Res 43: 514–525.

Chaudhuri RD, Banerjee D, Banik A, Sarkar S (2020) Severity and duration of hypoxic stress differentially regulates HIF-1α-mediated cardiomyocyte apoptotic signaling milieu during myocardial infarction. Arch Biochem Biophys 690: 108430.

El-Ella DM (2022) Autophagy/apoptosis induced by geraniol through HIF-1α/BNIP3/Beclin-1 signaling pathway in A549 CoCl2 treated cells. Adv Pharm Bull 12: 155–162.

Giudici F, Lombardelli L, Russo E, Cavalli T, Zambonin D, Logiodice F, et al. (2019) Multiplex gene expression profile in inflamed mucosa of patients with Crohn's disease ileal localization: A pilot study. World J Clin Cases 7: 2463–2476.

Huang YG, Tao W, Yang SB, Wang JF, Mei ZG, Feng ZT (2019) Autophagy: novel insights into therapeutic target of electroacupuncture against cerebral ischemia/reperfusion injury. Neural Regen Res 14: 954–961.

Huang YG, Wang JF, Li-Peng DU (2019) Effect of puerarin on regulation of AMPK-m TOR signaling pathway to inhibit autophagy and alleviate focal cerebral ischemia reperfusion injury. Chin Trad Herbal Drugs 50: 3127–3133.

Lee DH, Park JK, Choi J, Jang H, Seol JW (2020) Anti-inflammatory effects of natural flavonoid diosmetin in IL-4 and LPS-induced macrophage activation and atopic dermatitis model. Int Immunopharmacol 89: 107046.

Li M, Gao WW, Liu L, Gao Y, Wang YF, Zhao B, et al. (2020) The Akt/glycogen synthase kinase-3β pathway participates in the neuroprotective effect of interleukin-4 against cerebral ischemia/reperfusion injury. Neural Regen Res 15: 1716–1723.

Ling J, Cai H, Lin M, Qi S, Du J, Chen L (2021) RTN1-C mediates cerebral ischemia/reperfusion injury via modulating autophagy. Acta Biochim Biophys Sin 53: 170–178.

Liu X, Zhang M, Liu H, Zhu R, He H, Zhou Y, et al. (2021) Bone marrow mesenchymal stem cell-derived exosomes attenuate cerebral ischemia-reperfusion injury-induced neuroinflammation and pyroptosis by modulating microglia M1/M2 phenotypes. Exp Neurol 341: 113700.

Liu XW, Lu MK, Zhong HT, Wang LH, Fu YP (2019) Panax Notoginseng Saponins attenuate myocardial ischemia-reperfusion injury through the HIF-1α/BNIP3 pathway of autophagy. J Cardiovasc Pharmacol 73: 92–99.

Mokhtari-Zaer A, Saadat S, Marefati N, Hosseini M, Boskabady MH (2020) Treadmill exercise restores memory and hippocampal synaptic plasticity impairments in ovalbumin-sensitized juvenile rats: Involvement of brain-derived neurotrophic factor (BDNF). Neurochem Int 135: 104691.

Saw CL, Rakshasbhuvankar A, Rao S, Bulsara M, Patole S (2019) Current practice of therapeutic hypothermia for mild hypoxic ischemic encephalopathy. J Child Neurol 34: 402–409.

Scatozza F, D'Amore A, Fontanella RA, DE Cesaris P, Marampon F, Padula F, et al. (2020) Toll-like receptor-3 activation enhances malignant traits in human breast cancer cells through hypoxia-inducible factor-1α. Anticancer Res 40: 5379–5391.

Shao ZQ, Dou SS, Zhu JG, Wang HQ, Wang CM, Cheng BH, et al. (2021) Apelin-13 inhibits apoptosis and excessive autophagy in cerebral ischemia/reperfusion injury. Neural Regen Res 16: 1044–1051.

Singla S, Iwamoto-Stohl LK, Zhu M, Zernicka-Goetz M (2020) Autophagy-mediated apoptosis eliminates aneuploid cells in a mouse model of chromosome mosaicism. Nat Commun 11: 2958.

Wang Y, Meng C, Zhang J, Wu J, Zhao J (2019) Inhibition of GSK-3β alleviates cerebral ischemia/reperfusion injury in rats by suppressing NLRP3 inflammasome activation through autophagy. Int Immunopharmacol 68: 234–241.

Wang Y, Zhang H, Zhang Y, Li X, Hu X, Wang X (2020) Decorin promotes apoptosis and autophagy via suppressing c-Met in HTR-8 trophoblasts. Reproduction 159: 669–677.

Xie Y, Liu J, Kang R, Tang D (2020) Mitophagy receptors in tumor biology. Front Cell Dev Biol 8: 594203.

Xing XS, Liu F, He ZY (2015) Akt regulates β-catenin in a rat model of focal cerebral ischemia-reperfusion injury. Mol Med Rep 11: 3122–3128.

Xu D, Kong T, Zhang S, Cheng B, Chen J, Wang C (2021) Orexin-A protects against cerebral ischemia-reperfusion injury by inhibiting excessive autophagy through OX1R-mediated MAPK/ERK/mTOR pathway. Cell Signal 79: 109839.

Yang L, Jia R, Ji Q (2019) Patchouli alcohol induces autophagy in human lung adenocarcinoma cells A549 via increasing ratio of LC3 protein II/I and down-regulating p62. Precision Med Res 1: 6.

Yao X, Yao R, Huang F, Yi J (2019) LncRNA SNHG12 as a potent autophagy inducer exerts neuroprotective effects against cerebral ischemia/reperfusion injury. Biochem Biophys Res Commun 514: 490–496.

Zhang Y, Liu D, Hu H, Zhang P, Xie R, Cui W (2019) HIF-1α/BNIP3 signaling pathway-induced-autophagy plays protective role during myocardial ischemia-reperfusion injury. Biomed Pharmacother 120: 109464.

Zhu J, Wang YF, Chai XM, Qian K, Zhang LW, Peng P, et al. (2020) Exogenous NADPH ameliorates myocardial ischemia-reperfusion injury in rats through activating AMPK/mTOR pathway. Acta Pharmacol Sin 41: 535–545.

Zhu L, Qi B, Hou D (2019) Roles of HIF1α-and HIF2α-regulated BNIP3 in hypoxia-induced injury of neurons. Pathol Res Pract 215: 822–827.